Published OnlineFirst December 15, 2016; DOI: 10.1158/0008-5472.CAN-16-1387

Microenvironment and Immunology

Cancer Research

Early Effector T Lymphocytes Coexpress Multiple Inhibitory Receptors in Primary Non–Small Cell Lung Cancer

Elena Tassi[1], Giulia Grazia[1], Claudia Vegetti[1], Ilaria Bersani[1], Giulia Bertolini[2], Alessandra Molla[1], Paola Baldassari[1], Francesca Andriani[2], Luca Roz[2], Gabriella Sozzi[2], Ugo Pastorino[3], Roberta Mortarini[1], and Andrea Anichini[1]

Abstract

Clinical efficacy of PD-1/PD-L1 targeting relies upon the reactivation of tumor-specific but functionally impaired PD-1^+ T cells present before therapy. Thus, analyzing early-stage primary tumors may reveal the presence of T cells that are not yet functionally impaired. In this study, we report that activated (HLA-DR^+) T cells with an effector memory (T_{EM}) profile are enriched in such lesions. Tumor-infiltrating lymphocytes coexpressed PD-1 with the inhibitory receptors TIM-3, CTLA-4, LAG-3, and TIGIT, but also displayed a recently activated, nonexhausted phenotype. We also identified a subset of $CD8^+$PD-$1^+$$FOXP3^+$ T lymphocytes at the earliest phase of functional differentiation after priming, termed "early effector cells" (EEC), which also exhibited an activated nonexhausted phenotype, but was less differentiated and associated with coexpression of multiple inhibitory receptors. In response to autologous tumor, EECs upregulated CD107a, produced IL2 and IFNγ, and were competent for differentiation. The identification of EECs marked by inhibitory receptor expression at tumor sites will enable investigations of early stages of adaptive antitumor immunity, as well as support the rationale for administering immunotherapy in early-stage non–small cell lung cancer. *Cancer Res; 77(4); 851–61. ©2016 AACR.*

Introduction

Cancer immunotherapy by immune checkpoint blockade has shown remarkable clinical efficacy in several advanced tumors including melanoma, bladder cancer, and non–small cell lung cancer (NSCLC; ref. 1). In previously treated, advanced NSCLC patients, several phase II and III clinical trials with antibodies targeting the PD-1/PD-L1 axis have shown significant improvement in overall survival, compared with chemotherapy (2–5). Some studies have shown that clinical efficacy correlates with the level of expression of PD-1 ligand (PD-L1) on tumor cells or on tumor-infiltrating immune cells in pretherapy lesions (3, 4, 6). Interestingly, PD-L1 expression on tumor-infiltrating immune cells has also been shown to be associated with Th1-, T effector-, and IFNγ-associated gene signatures in the pretreatment neoplastic specimens (4, 6). This suggests that immunotherapy is effective in NSCLC patients with a preexisting T-cell–mediated immunity, negatively regulated by the PD-1/PD-L1 axis and rescued/reinvigorated by blocking this pathway. A similar interpretation has emerged from studies in melanoma and urothelial cancer (7, 8).

The spontaneous T-cell–mediated immune response likely begins to develop in early stages of tumor progression, fuelled by the accumulation of nonsynonymous somatic mutations, some of which may generate immunogenic neoantigens (9, 10). Indeed, neoantigen-specific T cells can be identified in early stage, primary NSCLC tissues, mainly from patients with a clonal neoantigen architecture of the lesion (10). Interestingly, these tumor-specific T cells coexpressed PD-1 and LAG-3 inhibitory receptors, but were also found to be positive for the proliferation marker Ki67 (10).

Constitutive upregulation of inhibitory receptors (IR, such as CTLA-4, PD-1, LAG-3, TIM-3, TIGIT, BTLA) by T cells (11, 12) can be a hallmark of functional impairment (exhaustion), and coexpression of multiple IRs, associated with T-cell dysfunction, has been correlated with tumor progression in NSCLC (13). Thus, one key question is whether IR^+ T cells at tumor site define only the chronically stimulated and functionally defective lymphocyte pool or rather they may also mark recently activated, proliferating, and functionally competent T cells. In fact, different IRs can be transiently expressed in the earliest phases of T-cell activation after priming, as shown in acute viral infection models (14). Recently activated T cells can be distinguished from chronically stimulated T lymphocytes by phenotypic and functional markers (14–18). Therefore, by looking at tumor tissues from early-stage primary tumors it should be possible to detect activated, functional IR^+ T cells at the beginning of the process leading to effector generation.

Here, we compared T-cell frequency and phenotype in the tumor and in matched non-neoplastic lung tissues (NnL) from

[1]Human Tumors Immunobiology Unit, Fondazione IRCCS Istituto Nazionale dei Tumori, Milan, Italy. [2]Tumor Genomics Unit, Department of Experimental Oncology and Molecular Medicine, Fondazione IRCCS Istituto Nazionale dei Tumori, Milan, Italy. [3]Unit of Thoracic Surgery, Fondazione IRCCS Istituto Nazionale dei Tumori, Milan, Italy.

Note: Supplementary data for this article are available at Cancer Research Online (http://cancerres.aacrjournals.org/).

R. Mortarini and A. Anichini contributed equally to this article.

Corresponding Authors: Andrea Anichini, Fondazione IRCCS Istituto Nazionale dei Tumori, Via Venezian 1, Milan 20133, Italy. Phone: 3902-2390-2817; Fax: 3902-2390-3237; E-mail: andrea.anichini@istitutotumori.mi.it; and Elena Tassi, elena.tassi@istitutotumori.mi.it

doi: 10.1158/0008-5472.CAN-16-1387

Published OnlineFirst December 15, 2016; DOI: 10.1158/0008-5472.CAN-16-1387

primary NSCLC surgical specimens. In the tumor tissue, we found an increased frequency of PD-1$^+$ T cells coexpressing multiple IRs, but retaining functional competence and expressing markers of recent activation. Among PD-1$^+$ T cells at tumor site, we also identified a subset of FOXP3$^+$CD8$^+$ "early effector T cells" (EEC), T lymphocytes at the first stage of differentiation after priming that express a CD127$^-$KLRG1$^-$CD27$^+$ profile distinct from naive cells and from subsequent functional fates (15, 17, 19). EECs found at tumor site in primary NSCLC upregulated multiple IRs, but retained competence for tumor recognition and for further differentiation. These IR$^+$ EECs provide a valuable biomarker for investigating the early phases of adaptive antitumor immunity in NSCLC.

Materials and Methods

Isolation of lymphocytes and cancer tissue–originated spheroids preparation

Lymphocytes were isolated from tumors and corresponding non-neoplastic lung specimens of American Joint Committee on Cancer (AJCC) stage IA–IV, histologically confirmed, primary NSCLC patients immediately after surgical removal. Informed consent was obtained from patients. Specimens were minced and treated by enzymatic digestion with collagenase IV (Sigma-Aldrich) and DNase I (Sigma-Aldrich) in RPMI1640 (BioWhittaker) for 1 hour at 37°C under agitation; digested tissues were passed through 100-μm and 40-μm cell strainers (Falcon, Corning Incorporated Life Sciences). Tissue fragments retained by the 40-μm cell strainer were collected and used to generate cancer tissue–originated spheroids (CTOS) as described by Endo and colleagues (20); CTOSs were kept in culture in DMEM F-12 (BioWitthaker) containing EGF (PeproTech, 20 ng/mL), bFGF (PeproTech, 20 ng/mL), B27 supplement minus vitamin A (Gibco, Life Technologies, 1×), and heparin sodium (Hospira, 0.6 IU/mL). After culture for 2 to 8 days, CTOSs were dissociated with Accumax (GE Life Sciences/PAA Laboratories) for 20 minutes at 37°C before use in coculture experiments. Cells in the flow-through fraction, not retained by the 40-μm cell strainer, were collected and red blood cells were removed by a solution containing NH_4Cl 0.15 mol/L, $KHCO_3$ 10 mmol/L and Na_2EDTA 100 mmol/L; the remaining cells were either immediately used for multiparametric flow cytometry characterization or frozen for subsequent analysis and experiments.

Flow cytometry

Multicolor staining of T lymphocytes and of dissociated CTOSs was performed as described previously (17, 20), with the antibodies listed in Supplementary Table S1. Staining of T cells was performed from cryopreserved samples subsequently thawed in the presence of DNase I. Briefly, 2×10^6 lymphocytes were resuspended in 100 μL of staining buffer (PBS plus 2% FBS) and stained for 30 minutes at +4°C with antibodies for cell surface markers; after wash, cells were permeabilized when needed with the Foxp3/Transcription Factor Staining Buffer Set (Affimetrix eBioscience) according to manufacturer's instructions, stained for intracellular molecules for 30 minutes at +4°C, washed, and acquired. Cells were analyzed by a four-color FACSCalibur (BD Biosciences) or a 10-color Gallios (Beckman Coulter) cytometers, and data were analyzed with FlowJo software (FlowJo, LLC). For analysis, data were gated on live cells, after excluding doublets (on SSC-A vs. SSC-H dot plots).

Immunohistochemistry

IHC was performed on formalin-fixed, paraffin-embedded (FFPE) tissues as described previously (17), using antibodies to CD3 (clone PS1, Novocastra), CD8 (clone C8/144B; Dako), PD-1 (clone NAT105; Biocare Medical), PD-L1 (clone SP142; Spring Biosciences), and to HLA class I (clone EMR8-5; Abcam). Two-color IHC was performed as described previously (17) with FOXP3-specific mAb (Abcam) followed by biotin-conjugated secondary anti-mouse antibody (Dako) and then by horseradish peroxidase–conjugated avidin (Dako). Sections were then stained with CD8-specific mAb (Dako) followed by polyclonal rabbit anti-mouse immunoglobulins (Dako) and by tertiary APAAP mAb (Dako). Development was done with Fast Red Substrate System (Dako). Isotype control antibodies matching CD8 Ab and FOXP3 Ab were clone DAK-GO1 (Dako) and ICIGG1 (Abcam), respectively. Images were acquired with an Axiovert 100 microscope (Zeiss; Carl Zeiss) equipped with a digital camera (AxioCam MrC5; Zeiss) or with an Aperio Scanscope XT digital pathology slide scanner (Leica Biosystems).

Functional assays

Tumor-associated lymphocytes (TAL) from digested tumor specimens were incubated overnight (18 hours) in the presence of autologous neoplastic cells from dissociated CTOS (lymphocytes:CTOS ratio ranging from 2:1 to 4:1), or phorbol 12-myristate 13-acetate (PMA; Sigma-Aldrich, 20 ng/mL) and ionomycin (Sigma-Aldrich, 500 ng/mL). In some experiments, neoplastic cells were preincubated with purified IgG2b or anti-CD274 (PD-L1) blocking antibody (BioLegend, 10 μg/mL). The experiments were performed in RPMI1640 containing 10% pooled human serum from healthy donors, in the presence of PE-CD107a (10 μl/mL); GolgiStop (BD Biosciences) was added 1 hour after the beginning of the culture. After coculture, the cells were collected and stained as described above. Intracellular IFNγ and IL2 were detected after permeabilization with the Foxp3/Transcription Factor Staining Buffer Set. For some experiments TALs were stained with CFSE (Molecular Probes) and then cultured with autologous tumor cells with/without IL2 (Chiron, 300 IU/mL) as described previously (17). Medium was changed and IL2 was replenished after 3 days; after 6 days, cells were stained as described previously (17). Separation of PD-1^{hi} and PD-1^{lo} fractions from TAL was carried out by staining with PE-conjugated anti PD-1 antibody (BD Biosciences), followed by incubation with anti-PE MicroBeads (Miltenyi Biotec) and magnetic separation with autoMACS Separator (Miltenyi Biotec) according to manufactrurer's instructions.

Statistical analysis

Paired Student *t* test was used to compare frequency of different T lymphocyte subsets in tumor versus NnL, of CD107a, IFNγ, or IL2 expression in cultures stimulated with PMA/ionomycin or with tumor cells versus control cultures, or in lymphocyte subsets defined by differential expression of PD-1 or of FOXP3. Unpaired Student *t* test was used to compare T-cell frequencies in samples from adenocarcinoma versus squamous cell carcinoma patients. ANOVA followed by SNK posttest was used to compare frequency of different T-cell subsets in patients groups according to AJCC clinical stage. Survival analysis was done by the Kaplan–Meier method, and survival curves were compared by the log-rank test. The Friedman test and Dunn multiple comparison test were used when comparing multiple T-cell subsets defined by CCR7 versus CD45RA expression.

Published OnlineFirst December 15, 2016; DOI: 10.1158/0008-5472.CAN-16-1387

Results

Enrichment for HLA-DR$^+$–activated T cells with an antigen-experienced profile in the primary tumor from NSCLC patients

T-cell frequency and activation profile were evaluated by flow cytometry in single-cell suspensions isolated from surgical specimens of primary tumors and of matched autologous NnL tissues of 87 NSCLC patients (see Supplementary Table S2 for demographic and clinical data). The tumor tissue, compared with NnL, showed a significant increase in frequency of CD3$^+$ and CD8$^+$ T cells (Fig. 1A), and of activated (HLA-DR$^+$) CD8$^+$ and CD4$^+$ T cells (Fig. 1B). The selective enrichment in the tumor versus NnL tissue for activated HLA-DR$^+$ T cells (mainly in the CD8$^+$ fraction) and of CD3$^+$ T cells was confirmed in patients' subsets defined by tumor stage (stage I to III), adenocarcinoma (ADC) versus squamous cell carcinoma (SCC) histology, smoking status, and previous neoadjuvant chemotherapy (Fig. 1C–F; Supplementary Fig. S1A–S1D). HLA-DR$^+$CD8$^+$ and HLA-DR$^+$CD4$^+$ T cells at tumor site showed a predominant CCR7$^-$CD45RA$^-$ antigen-experienced, effector memory (T_{EM}) phenotype (Supplementary Fig. S2A), a profile that also characterized most of the bulk CD4$^+$ and CD8$^+$ T-cell populations in the tumor (Supplementary Fig. S2B). Compared with NnL, tumor samples also contained an increased fraction of CD4$^+$ and CD8$^+$ cells coexpressing CD69 and CD27, consistent with recent activation of CD69$^+$ tissue-resident T cells (21, 22), whereas no significant differences were found for CD69$^+$CD27$^-$ T resident memory cells (Supplementary Fig. S2C; refs. 16, 17). Taken together, these results indicate a selective enrichment in the primary tumor tissue for activated, antigen-experienced HLA-DR$^+$ T cells.

Tumor-reactive and functionally competent T cells in the tumor tissue in primary NSCLC

Lymphocytes from tumor site were evaluated for CD107a upregulation, IFNγ and IL2 production in response to either polyclonal stimulation or to autologous tumor cells. In response to PMA/ionomycin, both CD8$^+$ and CD4$^+$ T cells from the

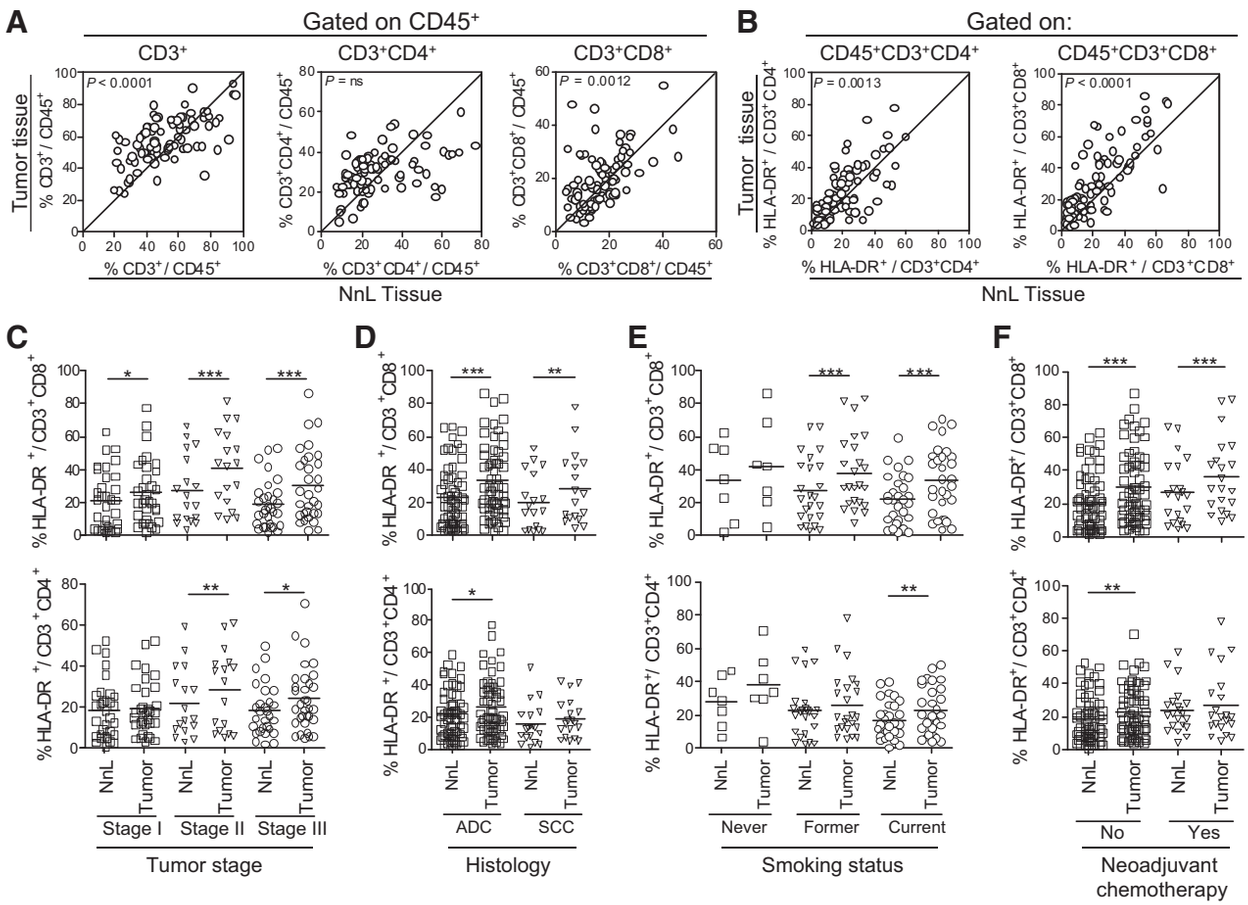

Figure 1.

Frequency of T cells and HLA-DR$^+$–activated T cells at tumor site compared with the corresponding NnL tissue in primary NSCLC. **A,** Flow cytometry analysis for frequency of CD3$^+$, CD3$^+$CD4$^+$, and CD3$^+$CD8$^+$ T cells, expressed as percentage of CD45$^+$ leukocytes, in single-cell suspensions from 87 NSCLC surgical specimens compared with the corresponding NnL tissue. **B,** Frequency of HLA-DR$^+$ cells in the CD4$^+$ ($n = 78$) and CD8$^+$ ($n = 82$) T-cell subsets in the tumor tissue compared with NnL as in **A**. **C–F,** Frequency of HLA-DR$^+$ cells in the CD8$^+$ (top) and CD4$^+$ (bottom) T-cell subsets in the tumor tissue compared with NnL, according to tumor stage (**C**; stage I, $n = 34$; stage II, $n = 18$; stage III, $n = 33$), histology (**D**; ADC, adenocarcinoma, $n = 60$; SCC, squamous cell carcinoma, $n = 19$), smoking status (**E**; never, $n = 7$; former, $n = 24$; current, $n = 30$), or neoadjuvant chemotherapy (**F**; no, $n = 67$; yes, $n = 20$). Horizontal bars in **C–F**, mean values. Statistical analysis by Student paired t test (**A–F**). Significant differences in **C–F** are expressed as: *, $P < 0.05$; **, $P < 0.01$; ***, $P < 0.001$.

Published OnlineFirst December 15, 2016; DOI: 10.1158/0008-5472.CAN-16-1387

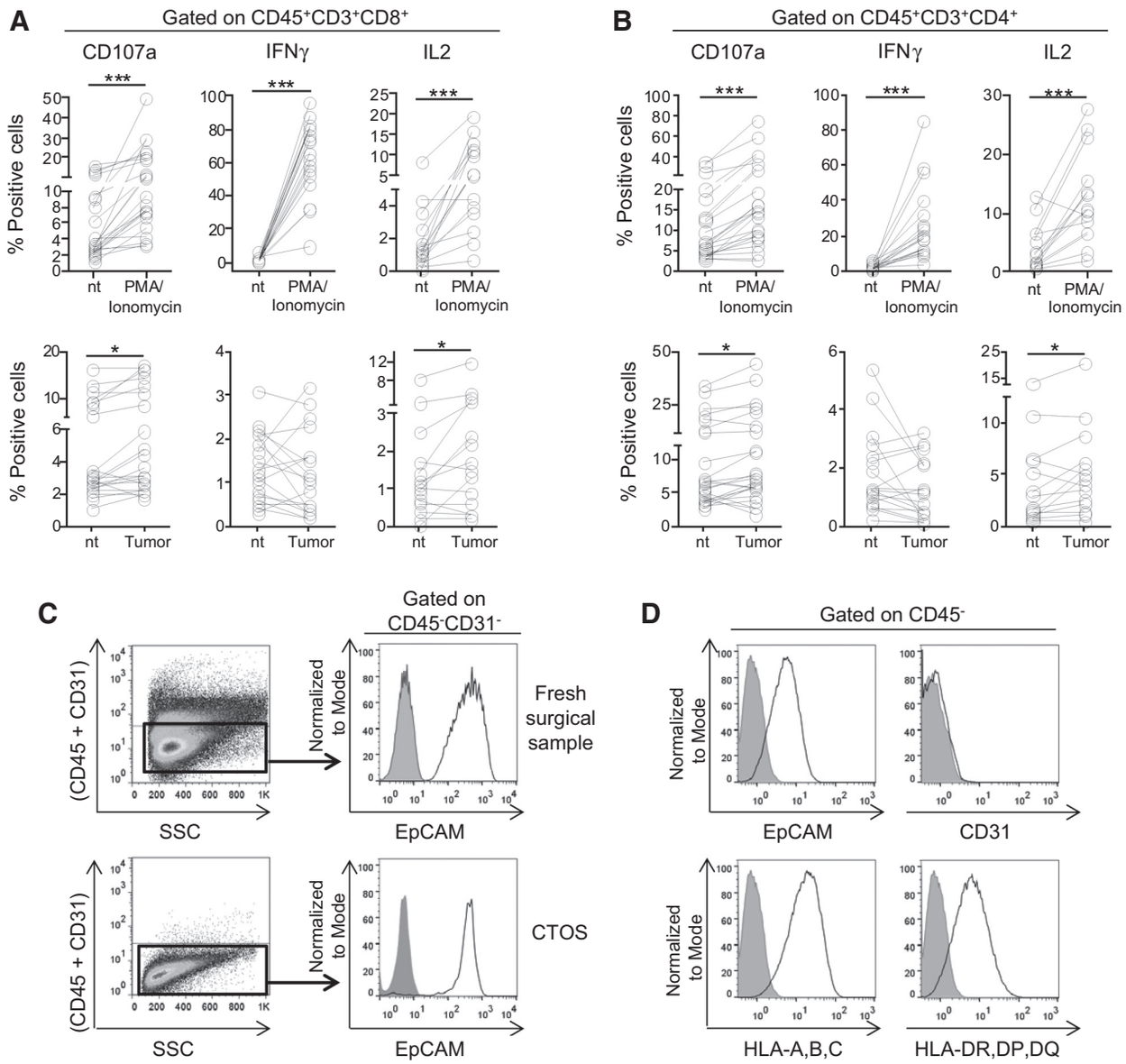

Figure 2.

Functional competence of T cells at tumor site in NSCLC. **A** and **B,** Surface expression of CD107a ($n = 21$), intracellular production of IFNγ ($n = 18$), or of IL2 ($n = 14$) by flow cytometry in $CD8^+$ (**A**) or $CD4^+$ (**B**) T cells, isolated from neoplastic tissue of primary NSCLC patients, in response to overnight stimulation with PMA plus Ionomycin (top graphs) or to overnight coculture with autologous tumor cells from dissociated CTOS (bottom graphs) in comparison with not treated (nt, i.e., lymphocytes cultured without PMA plus ionomycin or without autologous tumor cells). **C,** Identification of $CD45^-CD31^-EpCAM^+$ neoplastic cells by flow cytometry in single-cell suspension from a fresh NSCLC surgical sample. Cells were stained with PerCP-CD45, PerCP-eFluor710-CD31 (both detected through FL3 channel on a FACSCalibur cytofluorimeter), and FITC-EpCAM mAbs. Top, digested tissues at day 0, after filtering through a 40-μm cell strainer. Bottom, cells from the corresponding CTOS culture (at day +8). **D,** Flow cytometry analysis, after gating on $CD45^-$ cells, for EpCAM, CD31, HLA-A,B,C, and HLA-DR,DP,DQ (empty histograms) of cells dissociated from a CTOS culture at day +8. Gray histograms, cells stained with isotype control. Statistical analysis in **A** and **B** by Student paired *t* test. Significant differences are expressed as: *, $P < 0.05$; ***, $P < 0.001$.

neoplastic tissue of most patients upregulated CD107a and produced IFNγ and IL2 (Fig. 2A and B, top graphs). T-cell responsiveness to autologous tumor cells was evaluated using CTOSs generated from surgical specimens (20). Cancer cells dissociated from CTOSs showed a $CD45^-CD31^-EpCAM^+HLA\text{-}A,B,C^+HLA\text{-}DR^+$ profile (Fig. 2C and D for representative data on the phenotype of these cells). By IHC, HLA class I molecules were retained on neoplastic cells in the tissue sections corresponding to the surgical fragments used for obtaining CTOS ($n = 8$, data not shown). A low percentage of $CD8^+$ and $CD4^+$ T cells isolated from the neoplastic tissue were able to recognize autologous tumor upon coculture with CTOS-derived autologous tumor cells

Published OnlineFirst December 15, 2016; DOI: 10.1158/0008-5472.CAN-16-1387

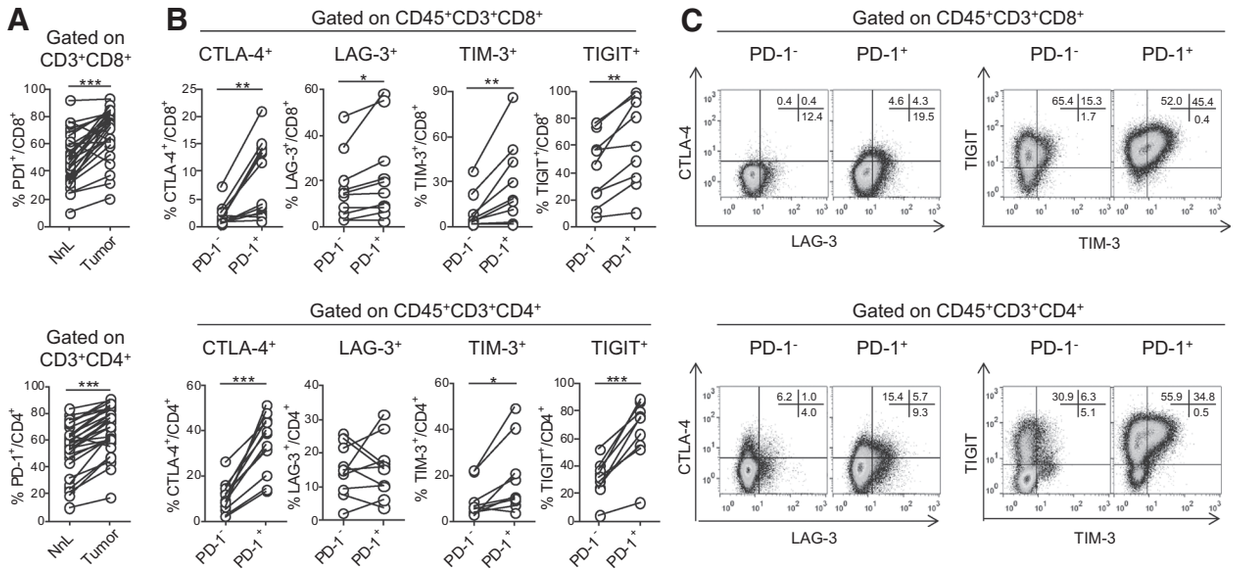

Figure 3.

Increased frequency of PD-1$^+$ T cells coexpressing additional inhibitory receptors in the tumor tissue compared with NnL tissue. **A,** Frequency of PD-1$^+$ cells in the CD3$^+$CD8$^+$ (top) and CD3$^+$CD4$^+$ (bottom) subsets in tumor tissues from 29 NSCLC surgical specimens compared with the corresponding NnL tissues. **B,** Frequency of CTLA-4$^+$ ($n = 12$), LAG-3$^+$ ($n = 10$), TIM-3$^+$ ($n = 9$), and TIGIT$^+$ ($n = 9$) T cells in the PD-1$^+$ and PD-1$^-$ fractions of CD3$^+$CD8$^+$ (top) or CD3$^+$CD4$^+$ (bottom) subsets at tumor site in NSCLC surgical specimens. Statistical analysis in **A** and **B** by paired Student *t* test. Significant differences are expressed as: *, $P < 0.05$; **, $P < 0.01$; ***, $P < 0.001$. **C,** Representative dot plots showing the expression of LAG-3 and CTLA-4 (left) or of TIM-3 and TIGIT (right) in the PD-1$^-$ and PD-1$^+$ subsets of CD3$^+$CD8$^+$ cells (top) or of CD3$^+$CD4$^+$ cells (bottom) from tumor site in a NSCLC surgical specimen. Numbers in the dot plots, percentage of cells in each quadrant.

(Fig. 2A and B, bottom graphs and Supplementary Fig. S3A for a representative experiment). This recognition was documented by CD107a mobilization assay (mean frequency of responding lymphocytes: 1.56%/CD8$^+$ and 2.45%/CD4$^+$) and intracellular IL2 production (mean frequency of responding lymphocytes: 0.98%/CD8$^+$ and 1.64%/CD4$^+$). In contrast, no significant IFNγ response was detected by CD4$^+$ or CD8$^+$ T cells upon coculture with autologous neoplastic cells (Fig. 2A and B, bottom graphs). Interestingly, IFNγ production in response to autologous tumor cells was observed by CD8$^+$ T lymphocytes upon inhibition of the PD-1/PD-L1 pathway with an anti-PD-L1–blocking antibody (Supplementary Fig. S3B). Control experiments indicated that PD-L1 blockade promoted the IFNγ response in T cells isolated from a PD-L1$^+$ tumor (Supplementary Fig. S3C, top), but not from a PD-L1$^-$ tumor (Supplementary Fig. S3C, bottom).

Activated and functional PD-1$^+$ T cells coexpressing multiple IRs are enriched in primary NSCLC

Frequency of PD-1$^+$ cells among CD8$^+$ and CD4$^+$ T cells was higher in the tumor tissue compared with matched NnL (Fig. 3A). In addition, the PD-1$^+$ fraction of both CD4$^+$ and CD8$^+$ T cells at tumor site showed enhanced expression of CTLA-4, LAG-3, TIM-3, and TIGIT IRs compared with PD-1$^-$ cells (Fig. 3B for all data and Fig. 3C for representative dotplots). CD4$^+$ and CD8$^+$ T cells expressing PD-1, or the other IRs (LAG-3, TIM-3, TIGIT) were found in AJCC stage I and II, early lesions, as well as in more advanced stage III tumors, but their frequency was not significantly associated with tumor stage or patients' survival (Supplementary Fig. S4A–S4C).

PD-1$^+$ T cells from the tumor, compared with NnL tissue, were enriched for Ki67$^+$ cells (i.e., proliferating) in both the CD8$^+$ and CD4$^+$ subsets (Fig. 4A and Supplementary Fig. S5B, left, for representative dotplots). Within the neoplastic tissue, and compared with the PD-1$^-$ T-cell fraction, PD-1$^+$CD8$^+$ and PD-1$^+$CD4$^+$ T cells showed a higher frequency of expression of proliferation (Ki67$^+$) and activation markers (CD137$^+$, CD38$^+$HLA-DR$^+$), associated with a less differentiated (mostly KLRG1$^-$CD127$^-$) profile (Fig. 4B and C) and with lack of expression of the exhaustion-related transcription factor Eomes (Supplementary Fig. S5B, middle and right, for representative results; ref. 18). A predominant Eomes-negative profile was found in all PD-1$^+$ CD8$^+$ T subsets from tumor site regardless of TIGIT and LAG-3 expression (Supplementary Fig. S6A–S6C).

In response to polyclonal stimulation, CD107a upregulation and production of IFNγ and IL2 were observed not only in the PD-1$^-$ T cell fraction, but even in PD-1$^+$CD4$^+$ and PD-1$^+$CD8$^+$ T lymphocytes, suggesting that the latter subsets were not functionally impaired (Fig. 4D). Polyclonal stimulation did not significantly affect the level of expression of PD-1 neither in the PD-1^{Lo} nor in the PD-1^{Hi} fractions obtained by magnetic separation from CD8$^+$ T cells from tumor site (Supplementary Fig. S7A and S7B). In addition, both the PD-1^{Lo} and the PD-1^{Hi} subsets in the CD8$^+$ cells produced IFNγ upon stimulation with PMA+ionomycin (Supplementary Fig. S7C and S7D). Furthermore, IFNγ production in response to polyclonal stimulation was retained in all PD-1$^+$ T-cell subsets from tumor site, irrespective of the coexpression of additional IRs (LAG-3, TIGIT, TIM-3; Supplementary Fig. S8A and S8B), although some significant differences were observed among the distinct subsets (Supplementary Fig. S8C).

Taken together, these results indicate selective enrichment at tumor site in primary NSCLC of IR$^+$ T cells that express a "recently activated" profile and retain functional competence.

Published OnlineFirst December 15, 2016; DOI: 10.1158/0008-5472.CAN-16-1387

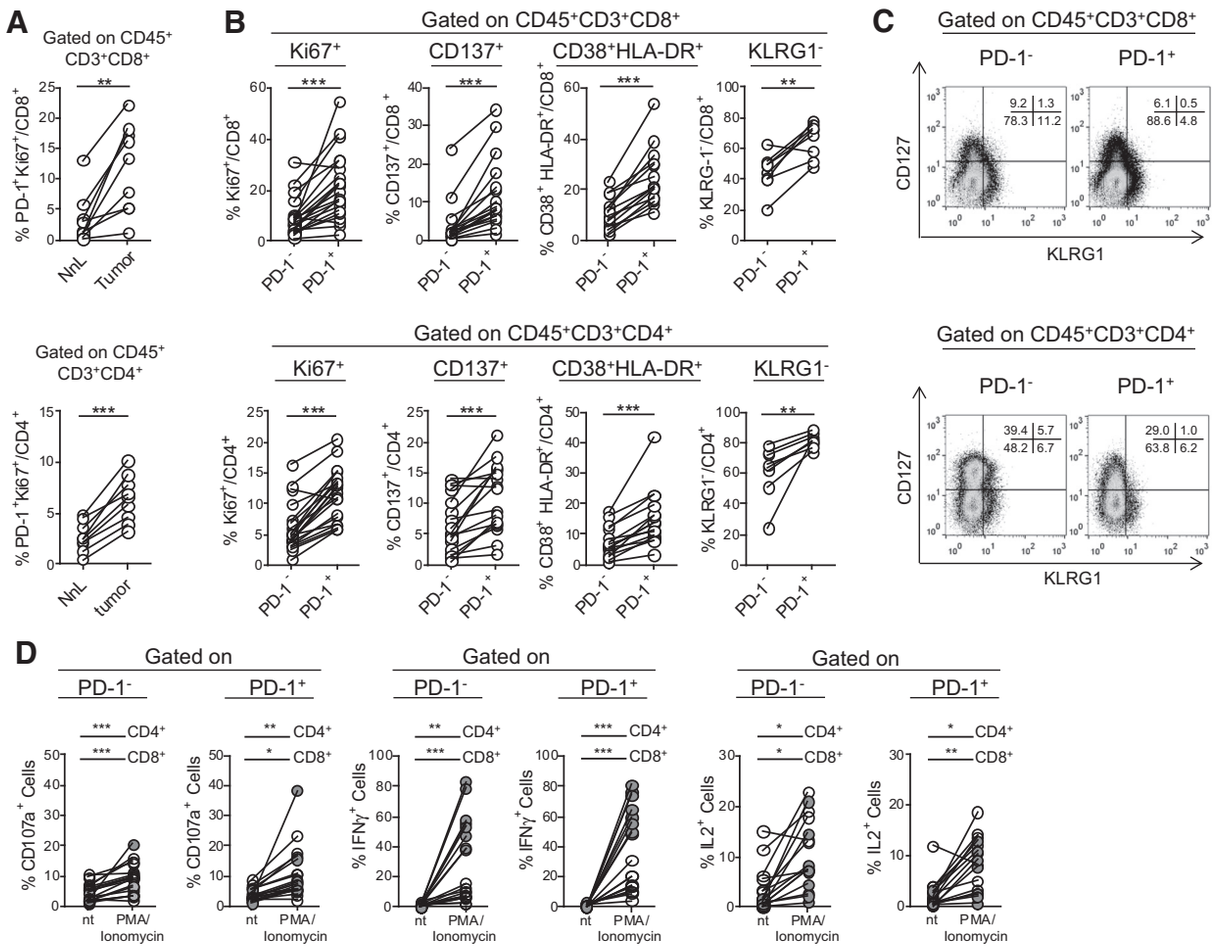

Figure 4.

Activation profile and functional competence of PD-1$^+$ and PD-1$^-$ T cells from tumor site in NSCLC. **A,** Frequency of PD-1$^+$Ki67$^+$ cells in the CD3$^+$CD8$^+$ (top graph) and CD3$^+$CD4$^+$ T-cell subsets in the tumor tissue compared with NnL tissue ($n = 9$). **B,** Frequency of Ki67$^+$ ($n = 21$), CD137$^+$ ($n = 17$), CD38$^+$HLA-DR$^+$ ($n = 15$), and KLRG1$^-$ ($n = 8$) cells in the PD-1$^-$ or PD-1$^+$ fractions of CD3$^+$CD8$^+$ (top) or of CD3$^+$CD4$^+$ (bottom) T lymphocytes in the tumor tissue. **C,** Representative staining for KLRG1 and CD127 in CD3$^+$CD8$^+$ (top) or CD3$^+$CD4$^+$ (bottom) T lymphocytes from tumor site of a NSCLC patient after gating on the PD-1$^-$ (left) or PD-1$^+$ (right) fractions. **D,** Upregulation of CD107a ($n = 9$; left), intracellular production of IFNγ ($n = 9$; middle) or IL2 ($n = 8$; right) in response to overnight stimulation with PMA/ionomycin in the PD-1$^-$ and PD-1$^+$ fraction of CD4$^+$ (empty symbols) or CD8$^+$ (gray symbols) subsets from tumor site.
Statistical analysis in **A**, **B**, and **D** by paired Student *t* test. Significant differences are expressed as: *, $P < 0.05$; **, $P < 0.01$; ***, $P < 0.001$.

Identification of CD8$^+$FOXP3$^+$ "early effector" T cells at tumor site coexpressing multiple IRs

The phenotypic traits of PD-1$^+$ T cells at tumor site were consistent with the profile of CD8$^+$FOXP3$^+$ EECs that we have previously identified in melanoma lesions (17), prompting the search for this subset even in NSCLC primary tumors. Indeed, a low frequency of CD8$^+$FOXP3$^+$ T cells was found in the tumor tissue of NSCLC patients (Fig. 5A for representative data). In tissue sections from NSCLC primary lesions, two-color IHC for CD8 and FOXP3 indicated, in most instances, that these two markers were expressed by distinct cells (Fig. 5B). However, CD8$^+$FOXP3$^+$ double positive cells could also be identified, often in direct contact with neoplastic cells (Fig. 5C, Supplementary Figs. S9B and S10C for data in three distinct patients; Supplementary Fig. S11A–S11E for high magnification images comparing single positive and double positive cells and Supplementary Figs. S12 and S13 for isotype control stainings). FFPE sections, corresponding to lesions from 10 different patients with a high (≥3%) frequency of CD8$^+$FOXP3$^+$/CD8$^+$, as assessed *ex vivo* by flow cytometry, were evaluated by IHC, revealing a stromal or intratumoral lymphocytic infiltrate positive for CD3, CD8, and PD-1 (Supplementary Figs. S14–S23). Interestingly, the same lesions also showed variable tumoral or stromal expression of PD-L1, often in the same areas containing PD-1$^+$ lymphocytes (Supplementary Figs. S14–S23).

By flow cytometry, CD8$^+$FOXP3$^+$ T cells, as well as CD8$^+$FOXP3$^+$CD25$^+$ T cells, were more frequent in the tumor, compared with NnL tissue (Fig. 5D). This selective enrichment of both CD8$^+$FOXP3$^+$ and CD8$^+$FOXP3$^+$CD25$^+$ T cells in the tumor versus NnL tissue was confirmed in patients subsets defined by histology, AJCC stage, smoking status, and neoadjuvant chemotherapy (Supplementary Fig. S24). CD8$^+$FOXP3$^+$ T-cell frequency was not significantly associated with tumor stage or with patients' survival (Supplementary Fig. S25), nor with type of

Published OnlineFirst December 15, 2016; DOI: 10.1158/0008-5472.CAN-16-1387

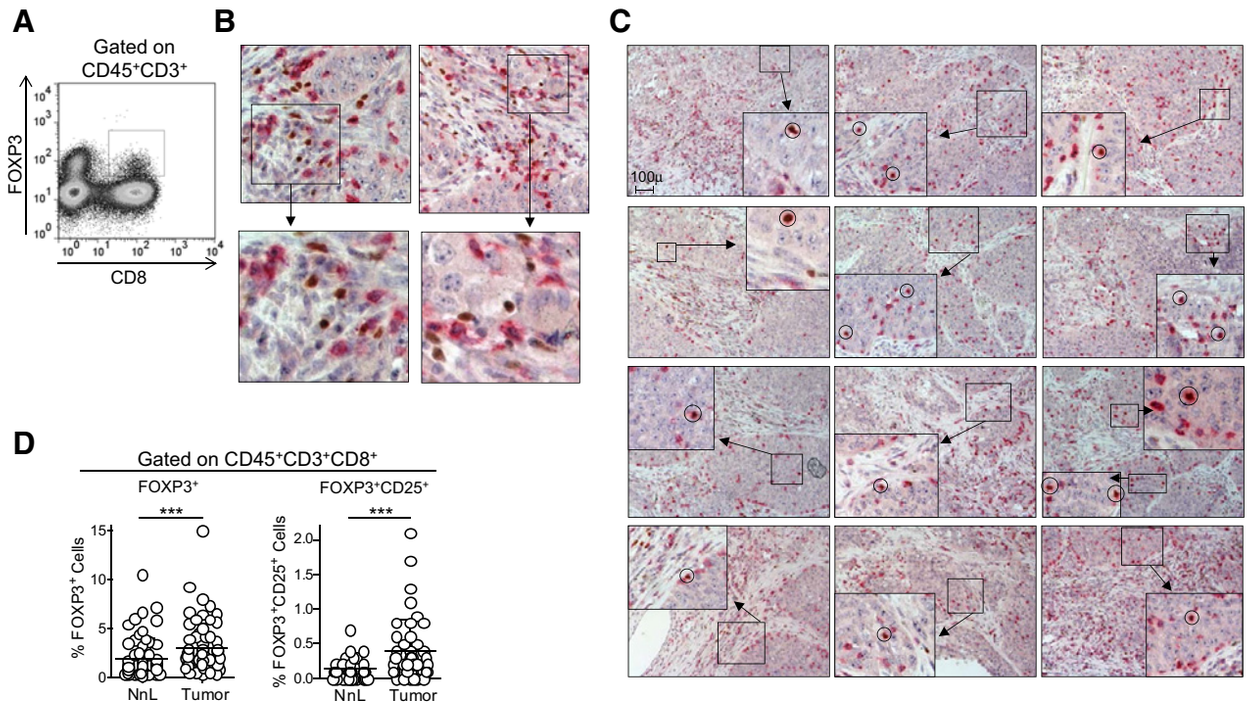

Figure 5.

Detection and frequency of CD8$^+$FOXP3$^+$ T cells at tumor site in NSCLC. **A,** Representative dot plot of T cells from tumor site of a NSCLC patient stained for CD8 and FOXP3 after gating on CD45$^+$CD3$^+$ cells. **B** and **C,** Sections from the neoplastic lesion of an adenocarcinoma patient containing intratumoral CD8$^+$ T-cell infiltrate were stained for FOXP3 (brown nuclear staining) and CD8 (purple cytoplasmatic and membrane staining). Single positive cells, staining only for CD8 or FOXP3 (**B**) and double positive cells staining for both CD8 and FOXP3 (**C**; circles and insets at higher magnification) were identified. Original magnification, ×20. **D,** Frequency, by flow cytometry, of FOXP3$^+$ (left; $n = 61$) and FOXP3$^+$CD25$^+$ (right; $n = 42$) cells in the CD3$^+$CD8$^+$ T-cell subset in the tumor tissue from NSCLC specimens compared with the corresponding NnL tissue. Horizontal bars, mean values. Statistical analysis by paired Student *t* test. Significant differences are expressed as: ***, $P < 0.001$.

therapy received in addition to surgery (namely neoadjuvant or adjuvant chemotherapy and/or radiotherapy; data not shown).

CD8$^+$FOXP3$^+$ T cells from tumor site expressed a predominant CCR7$^-$CD45RA$^-$ and CD127$^-$KLRG-1$^-$ profile (Supplementary Fig. S26A and S26B), in agreement with the expected profile of EECs (17). Within the neoplastic tissue, CD8$^+$FOXP3$^+$ T cells, when compared with CD8$^+$FOXP3$^-$ T lymphocytes, showed more frequent expression of CD25 and CD137, enrichment for CD25$^+$CD127$^-$ and for CD69$^+$CD27$^+$ cells, but lower fraction of CD69$^+$CD27$^-$ lymphocytes (Fig. 6A, top graphs), and increased frequency of perforin$^+$KLRG-1$^-$, Ki67$^+$, T-bet$^+$, and CD38$^+$HLA-DR$^+$ cells (Fig. 6A, bottom graphs). Thus, CD8$^+$FOXP3$^+$ T cells at tumor site express the expected "recently activated" phenotype of EECs that allows to distinguish this subset not only from naïve T cells (CD127^{hi}KLRG1^{lo}), but even from more advanced SLEC (CD127^{lo}KLRG1^{hi}CD27^{lo}) or MPEC (CD127^{hi}KLRG1^{lo}CD27^{hi}) fates (15, 17, 19). On the basis of the same sets of markers, CD8$^+$FOXP3$^+$ T cells at tumor site showed a more activated but less differentiated profile even when compared with the equivalent subset in NnL tissue and a lower expression of the senescent marker CD57 (Fig. 6B).

We then asked whether the EEC T-cell subset expressed or coexpressed several IRs. Compared with the CD8$^+$FOXP3$^-$ subset, CD8$^+$FOXP3$^+$ T cells at tumor site were characterized by a similar frequency of expression of PD-1, but more frequent expression of CTLA-4, TIM-3, LAG-3, and TIGIT (Fig. 7A), as well as by more frequent coexpression of PD-1 with CTLA-4, TIM-3, LAG-3, TIGIT, Ki67, and CD137 (Fig. 7B and C). Interestingly, expression and coexpression of IRs and of PD-1 with proliferation (Ki67) or activation (CD137) markers, but not with senescent (CD57) marker, were more frequent in CD8$^+$FOXP3$^+$ in the tumor tissue compared with CD8$^+$FOXP3$^+$ T cells in the NnL tissue (Supplementary Fig. S27A and S27B). Moreover, at tumor site, coexpression of CD38 with HLA-DR and of CD137 with Ki67 reached the highest levels in the CD8$^+$FOXP3$^+$PD-1$^+$ T cells, compared with the bulk CD8$^+$ or to the bulk CD8$^+$FOXP3$^+$ fractions (Supplementary Fig. S28A and S28B, values highlighted in red). Similarly, the fraction of T-bet$^+$ and Eomes$^-$ T cells was higher in the CD8$^+$FOXP3$^+$PD-1$^+$ T cells, compared with CD8$^+$ or to CD8$^+$FOXP3$^+$ fractions (Supplementary Fig. S28C for representative results).

By T-cell–CTOS coculture experiments, we then found that EECs from tumor site upregulated CD107a and also produced IFNγ and IL2 in response to autologous neoplastic cells, whereas the control CD4$^+$FOXP3$^+$T cells did not show such reactivity (Fig. 7D). In addition, CD8$^+$ FOXP3$^+$ EECs produced more IFNγ and IL2 in response to autologous tumor cells compared with matched CD8$^+$ FOXP3$^-$ subset (Fig. 7E). Finally, assessment of the potential of EECs for further differentiation was carried out in response to autologous tumor plus IL2, by CFSE dilution assay

Published OnlineFirst December 15, 2016; DOI: 10.1158/0008-5472.CAN-16-1387

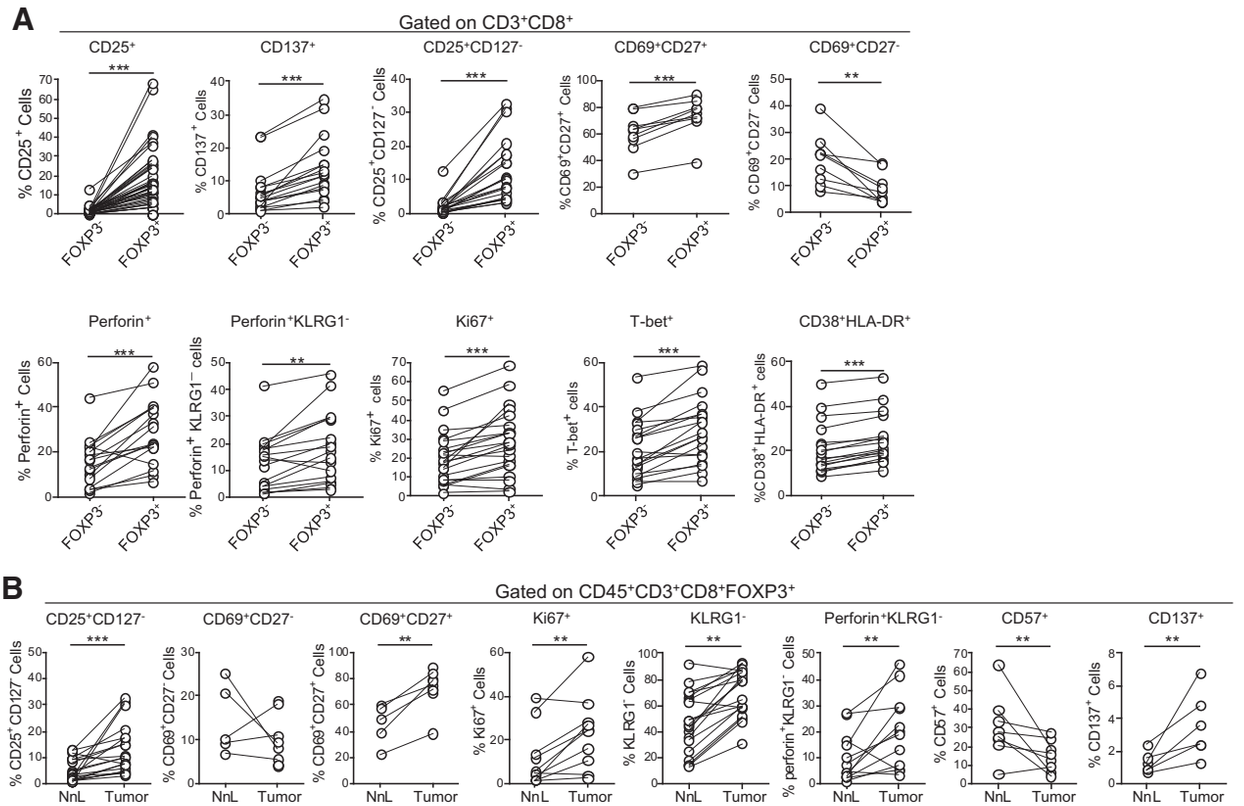

Figure 6.

Increased frequency of cells expressing an activated, "early effector" profile in the $CD8^+FOXP3^+$ T-cell subset at tumor site. **A,** Frequency of $CD25^+$ ($n = 45$), $CD137^+$ ($n = 17$), $CD25^+CD127^-$ ($n = 22$), $CD69^+CD27^+$ ($n = 9$), $CD69^+CD27^-$ ($n = 9$), $perforin^+$ ($n = 17$), $perforin^+KLRG1^-$ ($n = 17$), $Ki67^+$ ($n = 21$), $T\text{-}bet^+$ ($n = 19$), $CD38^+HLA\text{-}DR^+$ ($n = 17$) in the $CD8^+FOXP3^+$ versus $CD8^+FOXP3^-$ subsets at tumor site in NSCLC surgical specimens. **B,** Frequency of $CD25^+CD127^-$ ($n = 20$), $CD69^+CD27^-$ ($n = 5$), $CD69^+CD27^+$ ($n = 5$), $Ki67^+$ ($n = 10$), $KLRG1^-$ ($n = 19$), $perforin^+KLRG1^-$ ($n = 12$), $CD57^+$ ($n = 8$), $CD137^+$ ($n = 6$) in the $CD45^+CD3^+CD8^+FOXP3^+$ T lymphocytes in NSCLC tumor specimens compared with corresponding NnL tissues. Statistical analysis in **A** and **B** by paired Student *t* test. Significant differences are expressed as: **, $P < 0.01$; ***, $P < 0.001$.

coupled to analysis for CD27 and T-bet. Proliferating (i.e., $CFSE^-$) EECs (Supplementary Fig. S27C) showed decreased CD27 and increased T-bet expression (Supplementary Fig. S27D–S27E) consistent with ability of these cells for further differentiation (15, 23).

Taken together, these results indicate that the neoplastic tissue in primary NSCLC is enriched for functional, tumor-reactive $CD8^+FOXP3^+$ EECs that coexpress multiple IRs and retain competence for further differentiation.

Discussion

Primary NSCLC lesions can be infiltrated by T lymphocytes found in the stroma around tumor nests or within the tumor core (ref. 24, for review). Increased $CD3^+$ $CD8^+$ tumor-infiltrating lymphocytes (TIL), or the stromal $CD8^+$ T-cell density, are independent prognostic factors predicting better clinical outcome (25, 26). In addition, TILs in NSCLC tissues often display a memory phenotype (27, 28), with the evidence of activation (29, 30) suggesting that adaptive immune response to neoplastic cells takes place in some NSCLC patients.

A key question, addressed only in a few studies (30–32), is whether tumor-associated T cells are significantly enriched in the surgical tumor sample compared with matched NnL, because activated T cells can be found even in the non-neoplastic lung parenchyma (30, 32). In this study, we found a selective enrichment in the tumor for recently activated ($HLA\text{-}DR^+$) T cells expressing a T_{EM} profile compared with NnL. Interestingly, this enrichment was found even in AJCC stage I–II lesions and in tumors from current and former smokers, suggesting that some of the patients with early-stage lung cancer may have an active immune response, possibly fuelled by the high mutational burden occurring in smokers (9). Moreover, by functional assays, we found that both $CD4^+$ and $CD8^+$ subsets from the tumor tissue contained tumor-reactive effectors, as shown by the low frequency of lymphocytes that upregulate CD107a and produce IL2 in response to tumor cells.

T lymphocytes at tumor site, compared with NnL, showed an increased frequency of expression of PD-1, as well as of other IRs (CTLA-4, LAG-3, TIM-3, TIGIT). Coexpression of multiple IRs is a phenotypic feature associated with T-cell exhaustion in chronic viral infection models (14), in human HCV and HIV infections (33, 34) and in T cells at tumor site (13, 35–37). T-cell exhaustion is characterized by coexpression of several IRs (14), by upregulation of the transcription factor Eomes (18), and by reduced

Published OnlineFirst December 15, 2016; DOI: 10.1158/0008-5472.CAN-16-1387

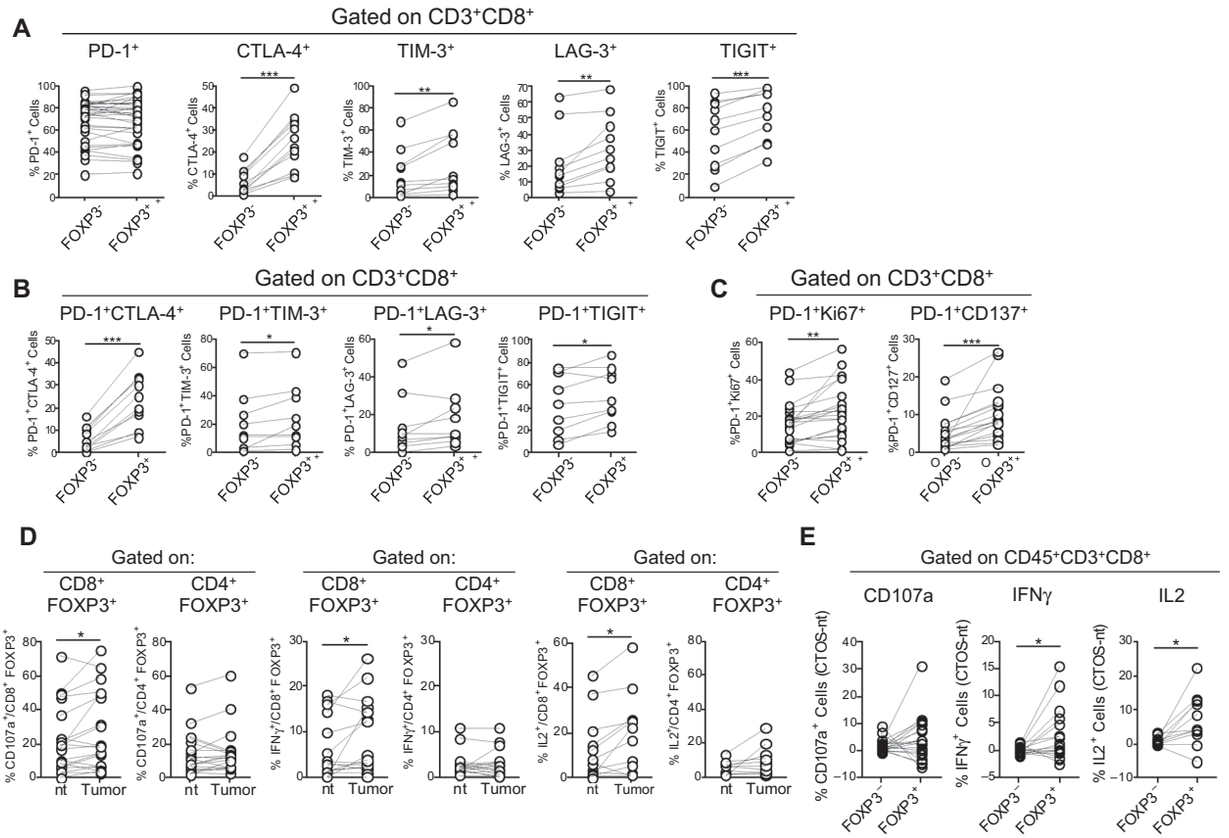

Figure 7.

Inhibitory receptors profile and functional competence of $CD8^+FOXP3^+$ EECs from tumor site in NSCLC. **A,** Frequency of PD-1^+ ($n = 35$), CTLA-4^+ ($n = 12$), TIM-3^+ ($n = 10$), LAG-3^+ ($n = 10$), and TIGIT$^+$ ($n = 10$) cells in the $CD8^+FOXP3^+$ versus $CD8^+FOXP3^-$ subsets at tumor site in NSCLC surgical specimens. **B** and **C,** Frequency of cells coexpressing PD-1 together with CTLA-4 ($n = 12$), TIM-3 ($n = 9$), LAG-3 ($n = 10$), TIGIT ($n = 9$), Ki67 ($n = 21$), or CD137 ($n = 17$) in the $CD8^+FOXP3^+$ versus $CD8^+FOXP3^-$ subsets at tumor site in NSCLC surgical specimens. **D,** Surface expression of CD107a ($n = 20$; left), intracellular production of IFNγ ($n = 16$; middle), and IL2 ($n = 12$; right) in $CD45^+CD8^+FOXP3^+$ or $CD45^+CD4^+FOXP3^+$ T cells from tumor site in response to overnight coculture with autologous tumor cells. **E,** Frequency of cells upregulating CD107a (left), producing IFNγ (middle) or IL2 (right) in response to overnight coculture with autologous tumor in the $FOXP3^+$ versus $FOXP3^-$ fractions of the $CD8^+$ T-cell subset from tumor site. Results are expressed as percent of positive cells in response to tumor after subtracting percent of positive cells in not treated cells. Statistical analysis in **A–E** by paired Student *t* test; significant differences are expressed as: *, $P < 0.05$; **, $P < 0.01$; ***, $P < 0.001$.

expression of the proliferation marker Ki67 and of the cytolytic factor Granzyme B (38). However, IRs can be transiently expressed at the early stages of T-cell activation after priming, as shown in acute viral infection models (14). We hypothesized that IR$^+$ T cells at tumor site in primary NSCLC could represent recently activated T cells at early stages of functional maturation after priming. In agreement, we found, at tumor site, IR$^+$ T cells with a recently activated and proliferating profile, associated with an early differentiation stage (KLRG-1^-CD127^-), and retaining functional competence in response to polyclonal stimuli.

We previously showed in melanoma that KLRG-1^-CD127^- $CD8^+$ T cells express FOXP3 and represent T lymphocytes at the earliest stage after priming (17). $CD8^+FOXP3^+$ T cells were enriched at tumor site even in NSCLC and showed the expected EEC profile ($CD127^-KLRG1^-CD27^+$), associated with a $CD45RA^-CCR7^-$ T_{EM} phenotype. These EECs were recently activated ($CD137^+$, $CD25^+$, $CD38^+HLA\text{-}DR^+$), proliferating cells ($Ki67^+$), with a nonexhausted profile (perforin$^+$, T-bet$^+$, Eomes$^-$, $CD57^-$), in spite of coexpression of several IRs (PD-1, CTLA-4, TIM-3, LAG-3, TIGIT). Moreover, $CD8^+FOXP3^+$ T lymphocytes were the only subset able to produce IFNγ after coculture with autologous neoplastic cells.

These findings suggest that early-stage neoplastic lesions are enriched for functional IR$^+$ EECs that transiently upregulate inhibitory receptors, whereas more advanced lesions may contain truly exhausted IR$^+$ T cells. Collectively, these results provide insight into the early phases of antitumor adaptive response in primary NSCLC and suggest that IR$^+$ $CD8^+$ EECs may represent a valuable biomarker for monitoring ongoing adaptive immunity to the tumor. Moreover, these results suggest that even early-stage primary NSCLC may be responsive to immunotherapy targeting immune checkpoints (2, 3), thus expanding the role of this therapeutic approach and improving the fraction of patients who may benefit from such therapeutic strategy.

Disclosure of Potential Conflicts of Interest

No potential conflicts of interest were disclosed.

Authors' Contributions

Conception and design: E. Tassi, G. Grazia, U. Pastorino, R. Mortarini, A. Anichini

Development of methodology: E. Tassi, C. Vegetti, G. Bertolini, A. Molla, P. Baldassari, F. Andriani, L. Roz, R. Mortarini

Acquisition of data (provided animals, acquired and managed patients, provided facilities, etc.): E. Tassi, G. Grazia, C. Vegetti, G. Bertolini, A. Molla, P. Baldassari, F. Andriani, G. Sozzi, U. Pastorino, A. Anichini

Analysis and interpretation of data (e.g., statistical analysis, biostatistics, computational analysis): E. Tassi, G. Grazia, C. Vegetti, A. Molla, P. Baldassari, L. Roz, R. Mortarini, A. Anichini

Writing, review, and/or revision of the manuscript: E. Tassi, G. Grazia, L. Roz, G. Sozzi, U. Pastorino, R. Mortarini, A. Anichini

Administrative, technical, or material support (i.e., reporting or organizing data, constructing databases): I. Bersani, P. Baldassari

Study supervision: R. Mortarini, A. Anichini

Grant Support

This work was supported by grant 17431 to A. Anichini from Associazione Italiana per la Ricerca sul Cancro (A.I.R.C., Milan) and by funds obtained through an Italian law that allows taxpayers to allocate 0.5% share of their income tax contribution to a research institution of their choice. E. Tassi was supported by Post-Doctoral Fellowships from Fondazione Umberto Veronesi, Italy. G. Grazia was supported by a Post-Doctoral Fellowship (#18202) from Fondazione Italiana per la Ricerca sul Cancro (FIRC), Milan, Italy.

The costs of publication of this article were defrayed in part by the payment of page charges. This article must therefore be hereby marked *advertisement* in accordance with 18 U.S.C. Section 1734 solely to indicate this fact.

Received May 13, 2016; revised November 12, 2016; accepted November 19, 2016; published OnlineFirst December 15, 2016.

References

1. Postow MA, Callahan MK, Wolchok JD. Immune checkpoint blockade in cancer therapy. J Clin Oncol 2015;33:1974–82.
2. Brahmer J, Reckamp KL, Baas P, Crino L, Eberhardt WE, Poddubskaya E, et al. Nivolumab versus docetaxel in advanced squamous-cell non-small-cell lung cancer. N Engl J Med 2015;373:123–35.
3. Borghaei H, Paz-Ares L, Horn L, Spigel DR, Steins M, Ready NE, et al. Nivolumab versus docetaxel in advanced nonsquamous non-small-cell lung cancer. N Engl J Med 2015;373:1627–39.
4. Fehrenbacher L, Spira A, Ballinger M, Kowanetz M, Vansteenkiste J, Mazieres J, et al. Atezolizumab versus docetaxel for patients with previously treated non-small-cell lung cancer (POPLAR): a multicentre, open-label, phase 2 randomised controlled trial. Lancet 2016;387:1837–46.
5. Herbst RS, Baas P, Kim DW, Felip E, Perez-Gracia JL, Han JY, et al. Pembrolizumab versus docetaxel for previously treated, PD-L1-positive, advanced non-small-cell lung cancer (KEYNOTE-010): a randomised controlled trial. Lancet 2016;387:1540–50.
6. Herbst RS, Soria JC, Kowanetz M, Fine GD, Hamid O, Gordon MS, et al. Predictive correlates of response to the anti-PD-L1 antibody MPDL3280A in cancer patients. Nature 2014;515:563–7.
7. Tumeh PC, Harview CL, Yearley JH, Shintaku IP, Taylor EJ, Robert L, et al. PD-1 blockade induces responses by inhibiting adaptive immune resistance. Nature 2014;515:568–71.
8. Rosenberg JE, Hoffman-Censits J, Powles T, van der Heijden MS, Balar AV, Necchi A, et al. Atezolizumab in patients with locally advanced and metastatic urothelial carcinoma who have progressed following treatment with platinum-based chemotherapy: a single-arm, multicentre, phase 2 trial. Lancet 2016;387:1909–20.
9. Rizvi NA, Hellmann MD, Snyder A, Kvistborg P, Makarov V, Havel JJ, et al. Cancer immunology. Mutational landscape determines sensitivity to PD-1 blockade in non-small cell lung cancer. Science 2015;348:124–8.
10. McGranahan N, Furness AJ, Rosenthal R, Ramskov S, Lyngaa R, Saini SK, et al. Clonal neoantigens elicit T cell immunoreactivity and sensitivity to immune checkpoint blockade. Science 2016;351:1463–9.
11. Blackburn SD, Shin H, Haining WN, Zou T, Workman CJ, Polley A, et al. Coregulation of $CD8^+$ T cell exhaustion by multiple inhibitory receptors during chronic viral infection. Nat Immunol 2009;10:29–37.
12. Wherry EJ, Kurachi M. Molecular and cellular insights into T cell exhaustion. Nat Rev Immunol 2015;15:486–99.
13. Thommen DS, Schreiner J, Muller P, Herzig P, Roller A, Belousov A, et al. Progression of lung cancer is associated with increased dysfunction of T cells defined by coexpression of multiple inhibitory receptors. Cancer Immunol Res 2015;3:1344–55.
14. Wherry EJ, Ha SJ, Kaech SM, Haining WN, Sarkar S, Kalia V, et al. Molecular signature of $CD8^+$ T cell exhaustion during chronic viral infection. Immunity 2007;27:670–84.
15. Joshi NS, Cui W, Chandele A, Lee HK, Urso DR, Hagman J, et al. Inflammation directs memory precursor and short-lived effector CD8(+) T cell fates via the graded expression of T-bet transcription factor. Immunity 2007;27:281–95.
16. Miller JD, van der Most RG, Akondy RS, Glidewell JT, Albott S, Masopust D, et al. Human effector and memory $CD8^+$ T cell responses to smallpox and yellow fever vaccines. Immunity 2008;28:710–22.
17. Anichini A, Molla A, Vegetti C, Bersani I, Zappasodi R, Arienti F, et al. Tumor-reactive $CD8^+$ early effector T cells identified at tumor site in primary and metastatic melanoma. Cancer Res 2010;70:8378–87.
18. Paley MA, Kroy DC, Odorizzi PM, Johnnidis JB, Dolfi DV, Barnett BE, et al. Progenitor and terminal subsets of $CD8^+$ T cells cooperate to contain chronic viral infection. Science 2012;338:1220–5.
19. Sarkar S, Kalia V, Haining WN, Konieczny BT, Subramaniam S, Ahmed R. Functional and genomic profiling of effector CD8 T cell subsets with distinct memory fates. J Exp Med 2008;205:625–40.
20. Endo H, Okami J, Okuyama H, Kumagai T, Uchida J, Kondo J, et al. Spheroid culture of primary lung cancer cells with neuregulin 1/HER3 pathway activation. J Thorac Oncol 2013;8:131–9.
21. Kaech SM, Cui W. Transcriptional control of effector and memory $CD8^+$ T cell differentiation. Nat Rev Immunol 2012;12:749–61.
22. Sathaliyawala T, Kubota M, Yudanin N, Turner D, Camp P, Thome JJ, et al. Distribution and compartmentalization of human circulating and tissue-resident memory T cell subsets. Immunity 2013;38:187–97.
23. Lefrancois L, Obar JJ. Once a killer, always a killer: from cytotoxic T cell to memory cell. Immunol Rev 2010;235:206–18.
24. Bremnes RM, Busund LT, Kilvaer TL, Andersen S, Richardsen E, Paulsen EE, et al. The Role of tumor-infiltrating lymphocytes in development, progression, and prognosis of non-small cell lung cancer. J Thorac Oncol 2016;11:789–800.
25. Schalper KA, Brown J, Carvajal-Hausdorf D, McLaughlin J, Velcheti V, Syrigos KN, et al. Objective measurement and clinical significance of TILs in non-small cell lung cancer. J Natl Cancer Inst 2015;107:pii: dju435.
26. Donnem T, Hald SM, Paulsen EE, Richardsen E, Al-Saad S, Kilvaer TK, et al. Stromal $CD8^+$ T-cell density: a promising supplement to TNM staging in non-small cell lung cancer. Clin Cancer Res 2015;21:2635–43.
27. Paulsen EE, Kilvaer T, Khanehkenari MR, Maurseth RJ, Al-Saad S, Hald SM, et al. CD45RO(+) Memory T lymphocytes–a candidate marker for TNM-immunoscore in squamous non-small cell lung cancer. Neoplasia 2015;17:839–48.
28. Djenidi F, Adam J, Goubar A, Durgeau A, Meurice G, de Montpreville V, et al. $CD8^+CD103^+$ tumor-infiltrating lymphocytes are tumor-specific tissue-resident memory T cells and a prognostic factor for survival in lung cancer patients. J Immunol 2015;194:3475–86.
29. Kataki A, Scheid P, Piet M, Marie B, Martinet N, Martinet Y, et al. Tumor infiltrating lymphocytes and macrophages have a potential dual role in lung cancer by supporting both host-defense and tumor progression. J Lab Clin Med 2002;140:320–8.
30. Marc MM, Korosec P, Kern I, Sok M, Ihan A, Kosnik M. Lung tissue and tumour-infiltrating T lymphocytes in patients with non-small cell lung carcinoma and chronic obstructive pulmonary disease (COPD): moderate/severe versus mild stage of COPD. Scand J Immunol 2007;66:694–702.
31. da Costa Souza P, Parra ER, Atanazio MJ, da Silva OB, Noleto GS, Ab'Saber AM, et al. Different morphology, stage and treatment affect immune cell

infiltration and long-term outcome in patients with non-small-cell lung carcinoma. Histopathology 2012;61:587–96.
32. Ganesan AP, Johansson M, Ruffell B, Yagui-Beltran A, Lau J, Jablons DM, et al. Tumor-infiltrating regulatory T cells inhibit endogenous cytotoxic T cell responses to lung adenocarcinoma. J Immunol 2013;191:2009–17.
33. Bengsch B, Seigel B, Ruhl M, Timm J, Kuntz M, Blum HE, et al. Coexpression of PD-1, 2B4, CD160 and KLRG1 on exhausted HCV-specific CD8$^+$ T cells is linked to antigen recognition and T cell differentiation. PLoS Pathog 2010;6:e1000947.
34. Peretz Y, He Z, Shi Y, Yassine-Diab B, Goulet JP, Bordi R, et al. CD160 and PD-1 co-expression on HIV-specific CD8 T cells defines a subset with advanced dysfunction. PLoS Pathog 2012;8:e1002840.
35. Fourcade J, Sun Z, Pagliano O, Chauvin JM, Sander C, Janjic B, et al. PD-1 and Tim-3 regulate the expansion of tumor antigen-specific CD8(+) T cells induced by melanoma vaccines. Cancer Res 2013;74:1045–55.
36. Gros A, Robbins PF, Yao X, Li YF, Turcotte S, Tran E, et al. PD-1 identifies the patient-specific CD8(+) tumor-reactive repertoire infiltrating human tumors. J Clin Invest 2014;124:2246–59.
37. Chauvin JM, Pagliano O, Fourcade J, Sun Z, Wang H, Sander C, et al. TIGIT and PD-1 impair tumor antigen-specific CD8$^+$ T cells in melanoma patients. J Clin Invest 2015;125:2046–58.
38. Twyman-Saint\sVictor C, Rech AJ, Maity A, Rengan R, Pauken KE, Stelekati E, et al. Radiation and dual checkpoint blockade activate non-redundant immune mechanisms in cancer. Nature 2015;520:373–7.

Cancer Research
The Journal of Cancer Research (1916–1930) | The American Journal of Cancer (1931–1940)

AACR American Association for Cancer Research

Early Effector T Lymphocytes Coexpress Multiple Inhibitory Receptors in Primary Non–Small Cell Lung Cancer

Elena Tassi, Giulia Grazia, Claudia Vegetti, et al.

Cancer Res 2017;77:851-861. Published OnlineFirst December 15, 2016.